International Food Research Journal 30(1): 163 - 172 (February 2023)
Journal homepage: *http://www.ifrj.upm.edu.my*

Clarification of red araçá (*Psidium cattleianum* Sabine) juice by membrane process: Analysis of permeate flux and loss of bioactive compounds

[1]Pinto, L. H. D., [2]Hamerski, F., [1]Scheer, A. P. and [1]*Silva, V. R.

[1]Department of Food Engineering, Federal University of Paraná, Av. Cel. Francisco H. dos Santos, Curitiba, Paraná, Brazil
[2]Depertment of Chemical Engineering, Federal University of Paraná, Av. Cel. Francisco H. dos Santos, Curitiba, Paraná, Brazil

Article history

Received:
12 April 2021
Received in revised form:
9 January 2022
Accepted:
9 June 2022

Keywords

Psidium cattleianum Sabine, phenolic content, antioxidant activity, porous membrane, fouling

Abstract

Red araçá (*Psidium cattleianum* Sabine) juice was processed using porous membranes to obtain a clarified product with a high amount of phenolic compounds prior to its use as a juice or other beverage. The variations in the permeate flux and concentrations of phenolics were determined in a cross-flow system using a polyetherimide microfiltration membrane (0.44 µm) and polyethersulfone ultrafiltration membrane (50 kDa). Both membranes reduced the initial turbidity (445 ± 2) to almost zero, and resulted in a clear and transparent permeate with a yellow colour. The microfiltration membrane showed better performance with the lowest phenolic compound retention (23.6%) and the highest permeate flux (40.6 ± 2 kg/m^{2}h) in batch mode operation. The permeate flux of the microfiltration system showed an initial sharp decrease followed by a gradual decrease, reaching almost 60% lower than the initial permeate flux. The permeate flux resistance was mainly due to the polarised layer (70.2%), and the predominant fouling mechanism was the partial pore blockage, thus indicating that the solids present in the raw juice had size of the same order as the membrane pores.

DOI
https://doi.org/10.47836/ifrj.30.1.13

Introduction

Brazil is known for its great diversity of native fruit trees, notably the species of the Myrtaceae family. This family includes the genus *Psidium* which has a wide distribution within the Brazilian territory. Red araçá fruit (*P. cattleianum* Sabine) has a firm, sweet, and acid pulp, and is highly appreciated for its exotic flavour. It is usually obtained directly from the harvest in native vegetation or small orchards, and often marketed traditionally (Patel, 2012; Mallmann *et al*., 2020). Studies have shown that this fruit can reduce the development of degenerative diseases such as atherosclerosis, cancers, cardiovascular diseases, and diabetes, mainly attributed to the high content of phenolic compounds with high antioxidant capacity such as epicatechin and gallic acid (Medina *et al*., 2011; Pereira *et al*., 2018). This means it can protect biological systems against excess free radicals and reactive oxygen species, and also contributes to the pigmentation, astringency, and oxidative stability (Jacques and Zambiazi, 2011; Pereira *et al*., 2018; Lima *et al*., 2020). However, red araçá fruit is mostly consumed locally as a fresh fruit due to its high perishability. Therefore, the development of new technology is of interest to obtain new products, especially juices, to encourage its consumption (Santos *et al*., 2007).

In this context, membrane processes separation (microfiltration, MF; and ultrafiltration, UF) has been successfully applied in the fruit juice production process, especially in the clarification step. A superior quality of clarified fruit juice could make a strong impact in new market areas such as clear and fresh juices, beverage blends, liqueurs, and soft drinks, and also in all applications where suspended solids are undesirable on the final product quality (Oliveira *et al*., 2012; Ribeiro *et al*., 2018). In comparison to the conventional processes, MF and UF can bring the following benefits: separation can be carried out without changing the temperature and pH of the solution or the need for chemical additives, thus

*Corresponding author.
Email: vrenan@ufpr.br

reducing the production costs and solving the problem of waste treatment, improving the product quality, and reducing labour costs (Urošević *et al*., 2017). The major obstacle for the application of these processes in juice clarification is the rapid decline of the permeate flux over time due to fouling and concentration polarisation (Echevarria *et al*., 2011; Bhattacharjee *et al*., 2017).

The basic principle of crossflow membrane separation is an accumulation of the retained solute and depletion of the permeating components in the boundary layer over the membrane surface. This causes a concentration gradient to build up in the boundary layer, thus resulting in a diffusive flux in the opposite direction to the permeate flux, known as concentration polarisation (Bhattacharya and Hwang, 1997). Fouling occurs due to various physical interactions of the fruit juice components with the membrane such as mechanical pore obstruction, adsorption of solutes at the membrane surface, and cake layer formation (Echevarria *et al*., 2011). In fruit juice processing using MF or UF, the permeate flux decline is predominantly associated with the presence of cell-wall polysaccharides such as pectin, cellulose, lignin, and hemicellulose (Vaillant *et al*., 1999). An understanding of these phenomena and analysis of how they are associated with operational conditions allows the economic viability of the process since the permeate flow is a critical parameter.

In this context, the present work investigated the performance of the porous membrane process in the clarification of red araçá juice. The influence of different membrane materials and transmembrane pressures were evaluated in terms of the permeate flux and the loss of bioactive compounds. The permeate flux resistances and the identification of the predominant fouling mechanisms during the clarification process were also investigated.

Materials and methods

Materials

Red araçá fruits were harvested in Curitiba (Paraná, Brazil; 25°16’21.3’’S, 49°08’24.9’’W). The fruit samples were selected, washed, sanitised with sodium hypochlorite (2%, w/v) for 15 min, pulped, and sieved through size 8 mesh (pore size 2.38 mm; Chemist Ltda., São Paulo, São Paulo State, Brazil). The material obtained was stored in plastic packaging, and frozen at -18°C until analysis. All chemicals used were of analytical grade.

Red araçá crude extract

The crude aqueous extract of red araçá (raw juice) was obtained by applying the ultrasound-assisted solid-liquid extraction (UAE) process by placing 1,000 g of deionised water acidified with citric acid (0.1%, w/v) in a beaker with 50 g of red araçá pulp (5.0%, m/m). The UAE was performed in an ultrasonic washer (Eco-Sonics, model Q 5.9 L, ultrasonic power 200 Watts RMS, 40 kHz, São Paulo, Brazil) at 60°C for 120 min, using a mechanical stirrer (IKA, model RW 20, Germany) with constant agitation at 470 rpm. The pulp and larger solid particles were removed using a 200 mesh stainless steel sieve (pore size 0.075 mm). Deionised water acidified with citric acid (0.1%, w/v) was then added to the filtered extract to give a volume of 2 L of solution, which was subsequently submitted to the clarification process. The solution was cooled and used in the membrane separation tests.

Physicochemical analysis

The feed and permeate samples of red araçá juice processed by MF and UF were analysed for total phenolic content (TPC), total flavonoid content (TFC), total solid content (TSC), turbidity, antioxidant activity, and colour (dry). All measurements were performed in triplicate, and the results expressed as mean ± standard deviation.

The TPC was determined following Singleton *et al*. (1999). Absorbance was measured at 760 nm using a UV-Vis spectrophotometer (Global Analyzer). The results were expressed in gallic acid equivalents (mg GAE/100 g of fruit).

The TFC was determined following Zhishen *et al*. (1999). Absorbance was measured at 510 nm using a UV-Vis spectrophotometer (Global Analyzer). Catechin was used as a standard to obtain the calibration curve, and the results were expressed in mg of catechin equivalent (CE) per litre of extract (mg CE/L).

The TSC was determined following Adolfo Lutz Institute (2005) using the gravimetric technique which involved drying the sample (evaporating the water and volatile substances present). The total dry extract was determined from the difference in sample mass values before and after drying.

The turbidity was determined using a digital turbidimeter (PoliControl, model AP 2000). This equipment compares the scattering of a beam of light passing through the sample with the scattering of a

beam of equal intensity passing through a standard suspension.

The colour was determined using a colorimeter (MiniScan XE Plus, Hunter Associates Laboratory, USA), and classified based on the CIE system with three dimensions: redness/greenness (a*), yellowness/blueness (b*), and brightness/darkness (L*). The chroma (C*) and total colour difference (ΔE°) were calculated according to McLaren (1976).

The antioxidant activity was determined using ABTS, DPPH, and FRAP assays. The ABTS [2,2'-azino-bis(3-ethylbenzothiazoline-6-sulfonic acid] assay was performed following Re *et al*. (1999). The DPPH (2,2-diphenyl-1-picryl-hydrazil) radical scavenging ability assay was performed following Brand-Williams *et al*. (1995). The ferric-reducing antioxidant power (FRAP) was determined following Benzie and Strain (1996). The antioxidant activity was determined based on the Trolox calibration curve, and expressed as antioxidant capacity in Trolox equivalent (μmol) per litre of extract (μmol TE/L).

Clarification using membrane processes

Membrane processes were applied in the clarification of the red araçá crude extract using a laboratory-scale system. The membranes had a hollow fibre configuration, and a commercial polymeric cross-flow system (PAM Membranas Seletivas, Rio de Janeiro, Brazil) was used in the clarification by microfiltration with a polyetherimide membrane (MF-PEI, nominal pore diameter of 0.44 μm and surface area of 3.6 cm^2), and ultrafiltration with a polyethersulfone membrane (UF-PES, nominal molecular weight limit of 50 kDa and surface area of 3.6 cm^2).

The raw juice was initially processed in the total recycling mode, *i.e.*, the retentate and permeate were continuously recycled to the feed tank to ensure steady-state conditions in the volume and composition of the feed stream. This configuration was used to evaluate the effect of the transmembrane pressure on the permeate flux, and the rejection of phenolic compounds by each membrane. The membrane with the lowest loss of phenolic compounds was selected for the dynamic study, carried out in batch mode to evaluate the effect of transient conditions, and estimate the predominant fouling mechanism during the clarification of the red araçá juice. The batch mode process was operated at a temperature of 20°C, feed flow rate of 150 L/h, and the best transmembrane pressure was evaluated in the total recycling mode. Before and after the experiments with the raw juice, a study with deionised water was performed to measure the permeability of the membranes. After each essay, the red araçá juice was drained, and deionised water was fed to the system to evaluate the final permeability of the fouled membrane. The permeate flux was measured by the gravimetric method (Silva *et al*., 2012), using Eq. 1:

$$J_P(t) = \frac{M_{Permeate}}{t \cdot S} \quad \text{(Eq. 1)}$$

where, J_P = permeate flow rate (kg/m^2h), $M_{Permeate}$ = mass of clarified extract of red araçá accumulated in the permeate stream (kg) at time t (h), and S = membrane surface area (m^2).

The rejection coefficient (CR) for each parameter evaluated during the clarification process was determined using Eq. 2:

$$CR = \left(1 - \frac{c_P}{c_F}\right) \cdot 100 \quad \text{(Eq. 2)}$$

where, C_P and C_F = concentrations of a specific component available in permeate and feed, respectively.

The concentration factor (CF) is the ratio of the initial mass of the extract to the mass removed by filtration, and was obtained using Eq. 3:

$$CF = \left(\frac{M_O}{M_O - M_{Permeate}}\right) \cdot 100 \quad \text{(Eq. 3)}$$

where, M_O = initial batch mass (kg), and $M_{Permeate}$ = mass of clarified extract of red araçá accumulated in the permeate (kg) during the filtration time.

Chemical cleaning of the membrane was also carried out by leaving the membrane immersed in a 0.1 M NaOH solution for 24 h, followed by immersion in a 500 ppm NaClO solution for 1 h (Silva *et al*., 2012).

Resistance analysis

The series resistance model assesses the total contribution of the main components resistant to the permeate flux (J_p), described as a function of transmembrane pressure and total resistance (Gerke *et al*., 2017), and was obtained using Eq. 4:

$$J_P = \frac{TMP}{\mu \cdot R_T} \quad \text{(Eq. 4)}$$

where, TMP = transmembrane pressure (bar), R_T = total resistance, and μ = permeate viscosity. The total resistance is the sum of the resistances R_M, R_F, and R_P, and was obtained using Eq. 5:

$$R_T = R_M + R_F + R_P \quad \text{(Eq. 5)}$$

where, R_F = resistance due to fouling, R_M = membrane resistance, and R_p = resistance due to concentration polarisation. The value of R_m was obtained through the transmembrane pressure, the flux value obtained with water for the clean membrane (J_w) and the water viscosity (μ_j), using Eq. 6:

$$R_m = \frac{TMP}{J_w \cdot \mu_j} \quad \text{(Eq. 6)}$$

The fouling resistance (R_F) was determined with water permeate flux after the procedure with the red araçá extracts and the washing solution, using Eq. 7:

$$R_F = \frac{TMP}{J'_w \cdot \mu_j} - R_m \quad \text{(Eq. 7)}$$

where, J'_w = water permeate flux through the blocked membrane, and μ_w = water viscosity. Through the values obtained for R_T, R_M, and R_F, the value of the resistance due to concentration polarisation (R_P) was calculated using Eq. 5.

Identification of the fouling mechanism

The pore-blocking models were adopted to identify the predominant fouling mechanism. The general pore-blocking model can be described using Eq. 8 (Field *et al*., 1995):

$$\frac{dJ_p(t)}{dt} = -k_N \cdot \left(J_P - J_P^*\right) \cdot J_P^{2-N} \quad \text{(Eq. 8)}$$

where, k_N = experimental pore-blocking coefficient, J_P^* = ideal critical flux for which fouling does not occur (kg/m^{2}h), and N = experimental coefficient that determines the pore-blocking mechanism. The integration of Eq. 8 gave the distinct fouling mechanism models as a function of different values for the index (n).

Based on the complete pore-blocking model (n = 2.0), clogging occurs when the particle size of the solute is larger than the pore size of the membrane. The model considers that pore-blocking occurs over the membrane surface rather than inside the membrane pores. This can be described using Eq. 9:

$$J_p(t) = J_{LIM} + \left(J_O - J_{LIM}\right) \cdot \exp\left[-k_{2.0} \cdot t\right] \quad \text{(Eq. 9)}$$

The internal pore-blocking model (n = 1.5) describes the type of incrustation caused by particles smaller than the pores of the membrane. The adsorption or deposition in the internal cavities of molecules on the pore walls was obtained using Eq. 10:

$$J_p(t) = \frac{J_0}{\left(1 + J_0^{0.5} \cdot k_{1.5} \cdot t\right)^2} \quad \text{(Eq. 10)}$$

The intermediate model of pore-blocking (n = 1.0) assumes that the particle size is similar to the diameter of the pores present on the membrane surface. Thus, blockage occurs not only due to the deposition of molecules at the entrance of the pores but also to the deposition of molecules on those that have been deposited previously (Eq. 11).

$$J_P(t) = \frac{J_{LIM} \cdot J_O \cdot \exp\left[J_{LIM} \cdot k_{1.0} \cdot t\right]}{J_O \cdot \left(\exp\left[J_{LIM} \cdot k_{1.0} \cdot t\right] - 1\right) + J_{LIM}} \quad \text{(Eq. 11)}$$

The cake formation model (n = 0) characterises the formation of a polarised layer on the membrane surface, where the molecules are larger than the pore diameter, focusing both on the membrane surface and on the initially deposited layer of solids. Therefore, the resistance is related to the permeation due to the membrane plus the resistance produced by the filter cake, and was obtained using Eq. 12.

$$k_0 \cdot t = \frac{1}{J_{LIM}^{\,2}} \cdot \left[\ln\left(\frac{J_P(t)}{J_O} \cdot \frac{J_O - J_{LIM}}{J_P(t) - J_{LIM}}\right) - J_{LIM} \cdot \left(\frac{1}{J_P(t)} - \frac{1}{J_O}\right)\right] \quad \text{(Eq. 12)}$$

Eqs. 9 - 12 were subjected to non-linear least squares regression analysis at the 95% confidence interval. Levenberg-Marquart algorithm was employed and StatSoft STATISTICA (version 7.0, Tulsa, OK, USA) was used for all calculations. The residual sum of squares (RSS) and mean relative error (%) (MRE) were calculated for each model based on

Eqs. 13 and 14, respectively, where J_{EXP} and J_{CALC} were the values for the experimental and calculated permeate flux, respectively, and N_{EXP} was the number of experimental observations (experimental data points).

$$RSS = \sum_{N=1}^{n_{EXP}} \left[J_{CALC} - J_{EXP} \right]^2 \quad \text{(Eq. 13)}$$

$$MRE(\%) = \frac{\sum_{N=1}^{n_{EXP}} \left| \frac{J_{CALC} - J_{EXP}}{J_{EXP}} \right|}{N_{EXP} - 1} \cdot 100 \quad \text{(Eq. 14)}$$

Statistical analysis

All experiments were conducted in triplicate, and the results expressed as mean and standard deviation. The analysis of variance (ANOVA) was then performed, and Tukey's test was employed to compare the mean values with the 95% confidential interval. The software StatSoft STATISTICA (version 7.0, Tulsa, OK, USA) was also used for this analysis.

Results and discussion

Performance of microfiltration and ultrafiltration membranes

Table 1 shows the variation in the permeate flux of each membrane studied (MF-PEI and UF-PES) for the different transmembrane pressures (TMP) applied. The highest permeate flux values obtained using MF-PEI and UF-PES were 37.94 ± 1.54 and 23.21 ± 0.21 kg/m^{2}h, respectively, observed with the lowest transmembrane pressure evaluated (0.03 MPa). It can be observed that an increase in the transmembrane pressure from 0.03 to 0.11 MPa led to a decrease in the permeate flux in the case of MF-PEI, while for UF-PES, there was a smaller decrease in the permeate flux, based on the statistical analysis (ANOVA and Tukey's test with a significance level of 5%).

Table 1. Effect of transmembrane pressure on permeate flux for each membrane[1].

Transmembrane pressure (TMP) (MPa)	MF-PEI permeate flux (kg/m h)	UF-PEI permeate flux (kg/m h)
0.03	38.94 ± 1.54^{Aa}	23.21 ± 0.21^{Ba}
0.05	33.16 ± 0.48^{Ab}	22.62 ± 0.17^{Bb}
0.07	32.05 ± 0.57^{Ab}	22.54 ± 0.16^{Bbc}
0.09	31.19 ± 0.34^{Abc}	21.92 ± 0.07^{Bcd}
0.11	29.48 ± 0.03^{Ac}	22.18 ± 0.08^{Bbc}

Means followed by different uppercase superscripts in a row are significantly different by Tukey's test ($p < 0.05$). Means followed by different lowercase superscripts in a column are significantly different by Tukey's test ($p < 0.05$). [1]Total recycling mode: feed flow of 150 L/h and temperature of 20°C.

Table 2 reports the results of the physicochemical analysis and the turbidity removal for each membrane. The suspended solids showed a significant decrease in the permeates of the MF and UF membranes when compared with the feed samples, while the turbidity decrement were 99.6 and 99.8%, respectively, for MF and UF. These values showed the efficiency of the membranes in removing the solids present in the extract, thus decreasing the turbidity to close to zero, and the residual solids in the permeate were due to the soluble solids present as bioactive compounds and carbohydrates. Several authors have reported the efficiency of the porous membrane process in the removal of suspended solids from crude fruit extracts to obtain a clarified extract that can be used as a juice or a feedstock for beverage blends (Oliveira *et al*., 2012; Domingues *et al*., 2014; Santos *et al*., 2016; Conidi *et al*., 2017; Ghosh *et al*., 2017).

The TPC in the raw juice was 297.69 ± 2.73 mg GAE/100 g, that is, of the same order as that reported by other authors (Mallmann *et al*., 2020), while the samples of clarified juice obtained from the MF-PEI and UF-PES processes had TPC values of 227.55 ± 2.09 and 207.88 ± 3.55, respectively. The decrement was 23.5 and 30.3% for MF-PEI and UF-PES, respectively. This trend was also observed for the TFC, with decrement of 26.1 and 31.7% for MF-PEI and UF-PES, respectively. This loss of bioactive compounds may be associated with the physical and chemical affinities of the phenolic compounds with the surface of the membrane, as well as the interaction

of phenolic compounds with the suspended solids retained on the membrane surface, thus leading to the formation of complexes with an average size larger than the membrane pores. The partial retention of phenolic and flavonoid compounds may also be related to their adsorption on the membrane surface (Rouquié *et al*., 2019). Due to the lower amount of bioactive compounds in the permeate stream when compared with the raw juice, the antioxidant activity showed the same tendency, with decrement of 7.2 to 20%.

Aghdam (2015) reported a loss of phenolic content of around 36.4% during the clarification of pomegranate juice through microfiltration using a mixed-cellulose ester membrane, while Ribeiro *et al*. (2018) reported a loss of phenolic of 25% for clarified *umbu* juice with microfiltration ceramic membrane of 0.2 µm. Gerke *et al*. (2017) studied the clarification of *yerba-maté* extract with different types of membranes, and observed a high loss of phenolic compounds with hydrophilic MF membranes of α-alumina (almost 23%) and UF-PES (almost 18%), and the lowest loss of bioactive compounds with MF-PEI (almost 11%).

The clarified red araçá juice showed a change in colour, for both membranes evaluated, when compared with the raw juice, although the results obtained for the two membrane materials were statistically different from each other. The permeate luminosity (L*) showed a slight increase, while the chroma (C*) showed a slight decrease due to the suspended solids removal. The lower a* and b* values for the permeate suggested that the clarified juice had a more yellow tone. Some loss of colour (ΔE) can be explained by the natural colour of dye pigments being adsorbed onto the membrane (surface and internal pore membrane) and the suspended solids retained on the membrane (Rouquié *et al*., 2019). These physicochemical parameters demonstrated that the clarification using the membrane processes was efficient, providing a clear product with the desired yellow colour containing bioactive compounds.

The MF-PEI membrane was selected to evaluate the batch process since the loss of bioactive compounds and antioxidant activity was lower, and the permeate flux was higher when compared with the use of the UF-PES membrane.

Table 2. Physicochemical analyses for red araçá extract (raw juice) and those clarified by MF-PEI and UF-PES[1].

Parameter	Raw juice	MF-PEI permeate	UF-PES permeate
TSC[2]	4.18 ± 0.01[a]	0.17 ± 0.05[b]	0.13 ± 0.09[b]
Turbidity[3]	445.0 ± 1.0[a]	2.0 ± 0.5[b]	1.0 ± 0.5[b]
TFC[4]	81.85 ± 4.59[a]	60.48 ± 0.28[b]	55.93 ± 0.57[b]
TPC[5]	297.69 ± 2.73[a]	227.55 ± 2.09[b]	207.58 ± 3.55[c]
ABTS[6]	845.26 ± 2.32[a]	747.19 ± 3.03[b]	676.30 ± 5.71[c]
DPPH[6]	661.11 ± 2.49[a]	613.21 ± 6.45[b]	597.14 ± 7.39[b]
FRAP[6]	514.91 ± 2.11[a]	450.11 ± 3.80[b]	463.87 ± 14.86[b]
L*	47.80 ± 0.20[b]	49.48 ± 0.38[a]	49.48 ± 0.38[a]
a*	0.64 ± 0.05[a]	0.11 ± 0.09[b]	0.05 ± 0.06[b]
b*	6.94 ± 0.16[b]	4.75 ± 0.26[a]	4.77 ± 0.18[a]
C*	6.97	4.75	4.77
ΔE°	-	2.81	1.04
CR[7] - Turbidity (%)	-	99.6	99.8
CR[7] - TPC (%)	-	23.6	30.3
CR[7] - TFC (%)		21.6	31.7

Means followed by different lowercase superscripts in a row are significantly different by Tukey's test ($p < 0.05$). [1]Feed flow of 150 L/h at 20°C and transmembrane pressure of 0.03 MPa. [2]TSC = total solid content expressed as % w/w. [3]Turbidity = expressed as nephelometric turbidity units (NTU). [4]TFC = total flavonoid content expressed as mg of catechin equivalent (CE) per L (mg CE/L). [5]TPC = total phenolic content expressed as mg of gallic acid equivalent (GAE) per L (mg GAE/L). [6]Antioxidant activity = expressed as µmol Trolox per L (µmol/L). [7]CR = coefficient of rejection, (%) CR = (1 - $C_{PERMEATE}$ / C_{FEED}).

Batch process operation

The values for the permeate flux and rejection of total phenolic content (CR-TPC) during the clarification of red araçá juice in batch mode operation with the polyetherimide membrane (MF-PEI) are shown in Figure 1. The clarified red araçá juice showed a 100% reduction in turbidity, ensuring a juice free of suspended solids, which is desirable for the beverage industry (Echevarria *et al*., 2011). The phenolic compounds lost during the batch mode process varied between 29 and 21% of the same order, as that observed for the total recycling mode. The coefficient of rejection was higher in the first few minutes of batch operation, varying between 29 and 26%, due to the adsorption of phenolic content over the membrane surface before the formation of a polarised layer and a cake layer. After the dynamic resistances build-up, the rejection of phenolic compounds decreased when compared with the initial stage (around 22%), thus suggesting that their retention was solely due to the interaction of soluble phenolics with the suspended solids being retained over the membrane surface.

The permeate flux showed behaviour typical of crossflow filtration: the initial permeate flux (106.80 ± 4.16 kg/m^{2}h) showed an abrupt decrease at the initial stage, followed by a gradual and continuous decrease, thus resulting in a final permeate flux of 40.67 ± 0.48 kg/m^{2}h. The overall permeate flux decrease was 60% after 45 min with a concentrate factor of 2.2. The decrease in the permeate flux observed in the first 15 min of around 55% could be attributed to the polarised layer formation. After the polarised layer resistances stabilised, the permeate flux show a slower decrease toward a pseudo-steady state due to the increased built-up of cake and fouling resistances. Other authors have reported the same behaviour. Laorko *et al*. (2010) and Ennouri *et al*. (2015), for instance, reported decreases in the permeate flux of 70 and 95% in the clarification of pineapple juice (using a 0.3 µm pore diameter of hollow fibre polysulfone membrane) and purple carrot juice (with a 0.2 µm pore diameter of tubular ceramic membrane), respectively.

The decrease in the permeate flux over time observed during the red araçá juice clarification process could have been due to the interaction between the membrane and natural fouling agents, such as proteins, dietary fibres, non-soluble carbohydrates (cellulose and hemicellulose), and lignins. The average concentration of proteins in the mature red araçá fruit is reportedly around 4.0 g/100 g (dry matter), while the concentration of dietary fibres, non-soluble carbohydrates, and lignins are 12.0, 3.5, and 0.3 g/100 g, respectively. This indicates the presence of a large amount of fouling agents in red araçá raw juice, thus leading to a decrease in the permeate flux due to their retention by the membrane (Galho *et al*., 2007; Vriesmman *et al*., 2007; Pereira *et al*. 2018).

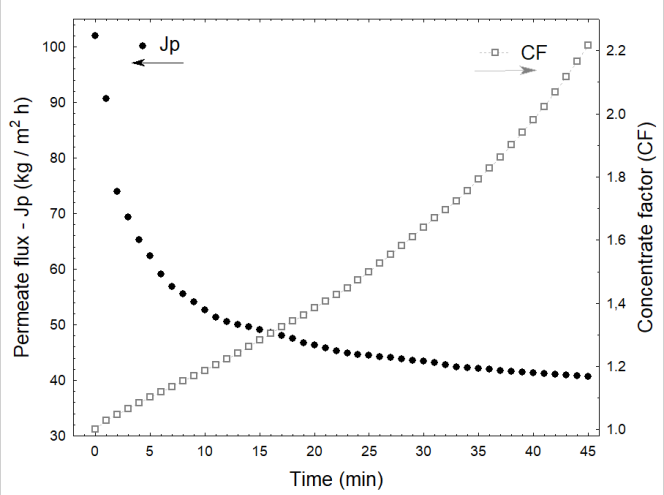

Figure 1. Clarification of red araçá extract with MF-PEI in batch mode operation: normalised permeate flux and coefficient of rejection for total phenolic content.

Analysis of resistances during the MF-PEI clarification in batch mode operation

Table 3 reports the absolute and relative contributions of the resistances during the clarification of the red araçá extract by microfiltration with the polymeric membrane (PEI) in batch mode operation (CF = 2.2).

Table 3. Estimated values of the resistance of the MF-PEI process in batch mode[1].

Resistance effect	Resistance	
	Absolute ($m^2/kg \times 10^{-1}$)	**Relative (%)**
Hydraulic membrane (R_M)	0.25	12.1
Fouling (R_F)	0.31	15.0
Polarized layer (R_P)	1.48	72.5
Total resistance (R_T)	2.04	100

[1]Operational parameters in MF-PEI: transmembrane pressure (TMP) = 0.03 MPa, T = 25°C, feed flow of 150 L/h. Concentrate factor of 2.2.

The polarisation resistance (R_P) had the highest index (72.5%), while the intrinsic membrane resistance (R_M) had the lowest (12.1%). This behaviour indicates that the effects of the concentration polarisation layer caused the accumulation of suspended solids over the membrane surface, thus leading to greater resistance to the passage of the flow than the sealing of the pores.

Ghosh *et al*. (2017) investigated the effect of the resistances in the clarification of *jamun* juice by microfiltration (hollow fibre membrane, polysulfone material, effective area 0.005 m^2). They also found that the greatest resistance was associated with the polarised layer, representing around 65% of the suspended solids deposition over the membrane surface and the dynamic resistance of the concentration polarisation layer.

To identify the predominant fouling mechanism, a comparative study between the experimental data and the predicted data obtained using models (Field *et al*., 1995) was carried out. The best fitting of the data was obtained with the partial pore-blocking model (R^2 = 98.03%, RSS = 250, and MRE = 3.3%). This model showed relative errors lower than 5% during the batch mode process time (Figure 2), thus indicating good prediction both in the initial stage (formation of concentration polarisation and the suspended solids deposition or cake layer formation) and in the pseudo-steady state.

Based on the partial pore-blocking model, the suspended particles are close to the pore size, and they tend the cluster in some regions of the membrane without closing it completely. This behaviour could be explained by the prior treatment of the crude aqueous araçá extract and the operational conditions in batch mode. Initially, the aqueous extract of red araçá was filtered through a 200 mesh stainless steel filter to remove large suspended particles and some fouling agents (dietary fibres and non-soluble carbohydrates such as cellulose and lignins), thus resulting in a juice with smaller suspended particles when compared with the crude red araçá extract. Some smaller molecules have, at first, a tendency to penetrate the membrane and accumulate inside the pores due to the effects of agglutination and adsorption (pigment retention on the inner walls of the membrane pores), while some larger particles tend to seal the external pore at the surface. Also, due to the low tangential velocity applied (0.13 $m.s^{-1}$ and Reynolds number close to 2570) and transmembrane pressure (0.03 MPa), the operation conditions prevented the formation of a compacted cake layer, but they did not prevent the surface deposition (due to the low shear rate stress), *i.e.*, the fouling occurred through a dynamic process involving the blocking/unblocking of pores. Similar behaviour was observed by Cassano *et al*. (2006), who identified partial pore-blocking as the predominant fouling mechanism in blood orange juice clarification using UF (tubular membrane, PVDF, 15 kDa), with a low Reynolds number (5800) and transmembrane pressure (0.85 MPa), while for a high Reynolds number (above 8000), the predominant fouling mechanism changes from partial to complete pore blocking.

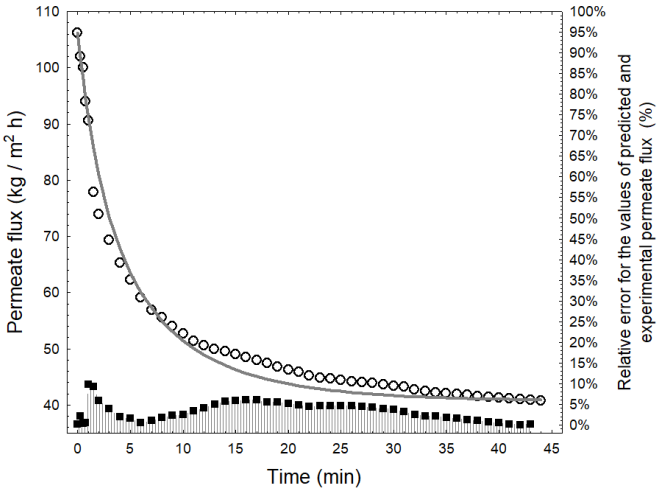

Figure 2. Fitting of the partial pore blocking (n = 1). (○) experimental data, (—) predicted data, and (■) relative error between predicted data and experimental data of permeate flux.

Conclusion

The present work demonstrated that red araçá juice had a considerable concentration of phenolic and flavonoid compounds. In addition, araçá extract exhibited high antioxidant activity. Additionally, the clarification process was efficient in removing the turbidity of the red araçá juice, which approached zero by applying the two membranes studied. Also, the permeate samples obtained showed clear appearance, and less intense colour. The microfiltration membrane (MF-PEI) showed a higher permeate flux (38.94 ± 1.54 kg/m^2h), and lower retention of phenolic and flavonoid compounds (23.5 and 26.1%) when compared with the ultrafiltration membrane (UF-PES), with corresponding values of 23.21 ± 0.21 kg/m^2h, 30.3 and 31.7%, respectively. The major factor associated with the resistance during

the clarification of the raw juice with MF-PEI was the polarised layer, accounting for around 70.2% of the total resistance. The fouling occurred predominantly through the partial pore-blocking mechanism. Results obtained in the present work contributed to applying the membrane process to clarify red araçá juice, thus resulting in a clarified juice with minimal loss of phenolic compounds. The use of this technology is attractive for the production of concentrated juice for use in the formulation of products with a high concentration of bioactive compounds and antioxidant activity.

Acknowledgement

The authors are grateful for the scholarship provided by CAPES, the research grant from the Graduation program of Food Engineering (Federal University of Paraná, Brazil), and the financial support received for the completion of the present work.

References

Adolfo Lutz Institute. 2005. Physico-chemical methods for food analysis. 4th ed. Brasília: Agência Nacional de Vigilância Sanitária.

Aghdam, M. A. 2015. The effect of ultrasound waves on the efficiency of membrane clarification of pomegranate juice. International Journal Food Science and Technology 50: 892-898.

Benzie, I. F. F. and Strain, J. J. 1996. The ferric reducing ability of plasma (FRAP) as a measure of antioxidant power: The FRAP assay. Analytical Biochemistry 239: 70-76.

Bhattacharjee, C., Saxena, V. K. and Dutta, S. 2017. Fruit juice processing using membrane technology: A review. Innovative Food Science and Emerging Technology 43: 136-153.

Bhattacharya, S. and Hwang, S. T. 1997. Concentration polarization, separation factor, and Peclet number in membrane processes. Journal of Membrane Science 132: 73-90.

Brand-Williams, W., Cuvelier, M. E. and Berset, C. 1995. Use of a free radical method to evaluate antioxidant activity. LWT - Food Science and Technology 28: 25-30.

Cassano, A., Marchio, M. and Drioli, E. 2006. Clarification of blood orange juice by ultrafiltration: Analyses of operating parameters, membrane fouling, and juice quality. Desalination 212: 15-27.

Conidi, C., Cassano, A., Caiazzo, F. and Drioli, E. 2017. Separation and purification of phenolic compounds from pomegranate juice by ultrafiltration and nanofiltration membranes. Journal of Food Engineering 195: 1-13.

Domingues, R. C. C., Ramos, A. A., Cardoso, V. L. and Reis, M. H. M. 2014. Microfiltration of passion fruit juice using hollow fiber membranes and evaluation of fouling mechanisms. Journal of Food Engineering 121: 73-79.

Echevarria, A. P., Torras, C., Pagán, J. and Ibarz, A. 2011. Fruit juice processing and membrane technology application. Food Engineering Reviews 3: 136-158.

Ennouri, M., Hassan, I. B., Hassen, H. B., Lafforgue, C., Schmitz, P. and Ayadi, A. 2015. Clarification of purple carrot juice: Analysis of the fouling mechanism and evaluation of the juice quality. Journal of Food Science and Technology 52: 2806-2814.

Field, R. W., Wu, D., Howell, J. A. and Gupta, B. B. 1995. Critical flux concept for microfiltration fouling. Journal of Membrane Science 100: 259-272.

Galho, A. S., Lopes, N. F., Bacarin, M. A. and Lima, M. G. S. 2007. Chemical composition and growth respiration in *Psidium cattleyanum* Sabine fruits during the development cycle. Revista Brasileira de Fruticultura 29: 61-66.

Gerke, I. B. B., Hamerski, F., Scheer, A. P. and Silva, V. R. 2017. Clarification of crude extract of yerba mate (*Ilex paraguariensis*) by membrane processes: Analysis of fouling and loss of bioactive compounds. Food and Bioproducts Processing 102: 204-212.

Ghosh, P., Rama, C. P. and Sabyasachi, M. 2017. Clarification of Jamun juice by centrifugation and microfiltration: Analysis of quality parameters, operating conditions, and resistance. Journal of Food Process Engineering 40: 12414.

Jacques, A. C. and Zambiazi, R. C. 2011. Phytochemicals in blackberry (*Rubus* spp). Semina - Ciências Agrarias 32: 245-260.

Laorko, A., Li, Z. Y., Tongchitpakdee, S., Chantachum, S. and Youravong, W. 2010. Effect of membrane property and operating conditions on phytochemical properties and

permeate flux during clarification of pineapple juice. Journal of Food Engineering 100: 514-521.

Lima, A. A., Maia, D. V., Haubert, L., Oliveira, T. l., Fiorentini, A. M., Rombaldi, C. V. and Silva, W. P 2020. Action mechanism of araçá (*Psidium cattleianum* Sabine) hydroalcoholic extract against *Staphylococcus aureus*. LWT - Food Science and Technology 119: 108884.

Mallmann, L. P., Tischer, B., Vizzotto, M., Rodrigues, E. and Manfroi, V. 2020. Comprehensive identification and quantification of unexploited phenolic compounds from red and yellow araçá (*Psidium cattleianum* Sabine) by LC-DAD-ESI-MS/MS. Food Research International 131: 108978.

McLaren, K. 1976. The development of the CIE 1976 (L* a* b*) uniform colour space and colour-difference formula. Journal of the Society of Dyers and Colourists 92: 338-341.

Medina, A. L., Haas, L. I. R., Chaves, F. C., Salvador, M., Zambiazi, R. C., Da Silva, W. P., ... and Rombaldi, C. V. 2011. Araçá (*Psidium cattleianum* Sabine) fruit extract with antioxidant and antimicrobial activities and antiproliferative effect on human cancer cells. Food Chemistry 128: 916-922.

Oliveira, R. C., Doce, R. C. and Barros, S. T. D. 2012. Clarification of passion fruit juice by microfiltration: analyses of operating parameters, study of membrane fouling and juice quality. Journal of Food Engineering 111: 432-439.

Patel, S. 2012. Exotic tropical plant *Psidium cattleianum*: A review on prospects and threats. Reviews in Environmental Science and Biotechnology 11: 243-248.

Pereira, E. S., Vinholes, J., Franzon, R. C., Dalmazo, G. M., Vizzotto, M. and Nora, L 2018. *Psidium cattleianum* fruits: A review on its composition and bioactivity. Food Chemistry 258: 95-103.

Re, R., Pellegrini, N., Proteggente, A., Pannala, A., Yang, M. and Rice-Evans, C. 1999. Antioxidant activity applying an improved ABTS radical. Free Radical Biology and Medicine 26: 1231-1237.

Ribeiro, L. O., Costa, S. D. O., Silva, L. F. M., Ferreira, J. C. S., Freitas, S. P. and Matta, V. M. 2018. Bioactive compounds and shelf life of clarified umbu juice. International Food Research Journal 25: 769-775.

Rouquié, C. Dahdouh. L., Ricci, J., Wisniewski, C. and Delalonde, M. 2019. Immersed membranes configuration for the microfiltration of fruit-based suspensions. Separation and Purification Technology 216: 25-33.

Santos, C. D., Scherer, R. K., Cassini, A. S., Marczak, L. D. F. and Tessaro, I. C. 2016. Clarification of red beet stalks extracts by microfiltration combined with ultrafiltration. Journal of Food Engineering 185: 35-41.

Santos, M. S., Petkowicz, C. L. O., Wosiacki, G., Nogueira, A. and Carneiro, E. B. 2007. Characterization of red araçá juice (*Psidium cattleianum* Sabine) mechanically extracted and enzymatically treated. Acta Scientiarum Agronomy 29: 617-621.

Silva, V. R., Hamerski, F. and Scheer, A. P. 2012. Pretreatment of aqueous pectin solution by cross-flow microfiltration: Analysis of operational parameters, degree of concentration and pectin losses. International Journal of Food Science and Technology 47: 1246-1252.

Singleton, V. L., Orthofer, R. and Lamuela-Raventos, R. M. 1999. Analysis of total phenols and other oxidation substrates and antioxidants by means of Folin-Ciocalteu reagent. Methods in Enzymology 299: 152-178.

Urošević, T., Povrenović, D., Vukosavljević, P., Urošević, I. and Stevanović, S. 2017. Recent developments in microfiltration and ultrafiltration of fruit juices. Food and Bioproducts Processing 106: 147-161.

Vaillant, F., Milan, P., O'Brien, G., Decloux, M. and Reynes, M. 1999. Crossflow microfiltration of passion fruit after partial enzymatic liquefaction. Journal of Food Engineering 42: 215-224.

Vriesmman, L. C., Petkowicz, C. L. O., Carneiro, P. I. B., Costa, M. E. and Beleski-Carneiro, E. 2007. Acidic polysaccharides from *Psidium cattleianum* (araçá). Brazilian Archives of Biology and Technology 52: 259-264.

Zhishen, J., Mengcheng, T. and Jianming, W. 1999. The determination of flavonoid contents in mulberry and their scavenging effects on superoxide radicals. Food Chemistry 64: 555-559.